Magnetism in CrI_3

Wietze Huisman

Supervisor: Dr M.K. Rösner
Day-to-day supervisor: Y. in 't Veld
Second corrector: Dr. N. Hauptmann

Institute for
Molecules and Materials
Radboud University

Theory of Condensed Matter
July 2021

Abstract

In this Bachelor Thesis, we give a minimalistic description of magnetism in monolayer CrI_3. This description is constructed from two seperate exchange interactions. We combine the antiferromagnetic Kugel-Khomski direct exchange, with the ferromagnetic Goodenough-Kanamori indirect exchange. In contrast to the individual models, the full model exhibits a magnetic phase transition. The near additive interplay between both exchange mechanisms allows for an insightful qualitative description of the magnetic properties. The predicted magnetic coupling of $J = 5.17$meV still strongly deviates from the actual value of $J \approx -1$meV. Therefore, on a quantitative level, the model is not fully reliable. However, the model still contains a number of approximations, which can heavily alter the quantitative result.

Contents

1 Introduction

In 2017, the first discovery of ferromagnetic ordering in a two-dimensional monolayer was made [1]. This discovery lead to a significant interest in the fundamentals of magnetism in such monolayers. The most popular of these materials being CrI_3. The first accurate description of this ferromagnetic ordering was proposed in 2019 [2]. This description is acquired via the magnetic force theorem. While this research has given an accurate and complete description of magnetism in CrI_3, the theory is generally very complex.

In this Bachelor Thesis we take a different approach. Starting from the Hubbard model, we will construct a minimal model describing the interactions within the CrI_3 lattice. In order for us to give a description of the magnetic properties, we will consider two interactions. First we present and explain the antiferromagnetic behaviour of the Kugel-Khomski direct exchange. This interaction represents the direct communication between the Chromium sites. Secondly, we will discuss the ferromagnetic behaviour of the Goodenough-Kanamori indirect exchange. In contrast to the direct exchange, this interaction is mediated by the Iodide ligands between the Chromium sites. These two exchange mechanisms will then be combined into a single model. The results of this model will be analysed. Especially the interplay between both exchange channels will be investigated.

The goal of this research is to qualitatively reproduce the results of previous research projects concerning CrI_3. By simulating this system in a minimalistic way, we hope to acquire a more insightful description of magnetism in CrI_3.

2 Theory

In this section, a brief overview of the relevant theory is given. We will introduce the researched material, discuss the applied model, and review the used software.

2.1 CrI_3

Figure 1 shows the lattice structure of CrI_3. The Cr^{3+} ions are surrounded by six I^- ions. These octahedrals form a honeycomb lattice, where two Chromium atoms are connected via two Iodide ligands. In this lattice, the valence shell of a Chromium site consists of d-orbitals, while the valence shell of an Iodide ligand consists of p-orbitals. Seeing as p-orbitals are lower in energy compared to the d-orbitals, we conclude that the Iodide ligands always contain fully occupied p-orbitals. As a result, the magnetization of the system is found via the spin-alignment on the partially filled d-orbitals of the Chromium sites.

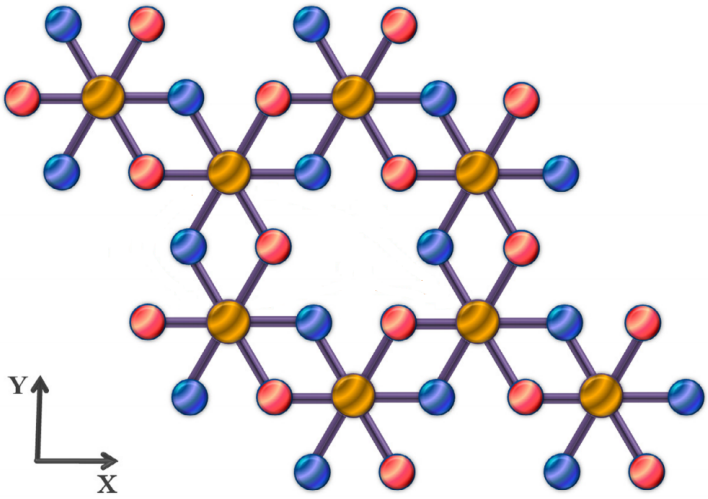

Figure 1: Schematic overview of the 2-dimensional lattice structure of monolayer CrI_3 [2]. The Chromium sites are presented in orange, while the intermediate iodide ligands are shown in red or blue.

In this research, we will only consider nearest neighbour interactions. Therefore, our full system will contain a single Cr-I-Cr chain. This is however still a two-dimensional system, where the angle of the ligand is of the utmost importance. This angle is calculated to be approximately 93° [3].

2.2 Hubbard Model

The Hubbard model describes quantum physics by considering possible configurations and transitions. This focus on configurations and transitions makes the use of second quantization operators highly effective. We can write any configuration or exchange mechanism in a mathematical form, simply by using the creation operator $\hat{a}^{\dagger}_{im\sigma}$ and the annihilation operator $\hat{a}_{im\sigma}$. Together, these operators construct the particle number operator: $\hat{n}_{im\sigma} = \hat{a}^{\dagger}_{im\sigma}\hat{a}_{im\sigma}$. In this notation, the index i enumerates the specific site at which the considered electron is placed. Additionally, the index m refers to the orbital on this site. Finally, σ can be either up or down, as it represents the spin of the considered electron.

A simple Hubbard model is the two-site model. This model contains two atoms (sites), where each atom contains a single orbital. The operator Hamiltonian for this model is given by equation 1. In this Hamiltonian, the indices i and j run over the two sites. All parameters in this equation will be explained below.

$$\begin{aligned}\hat{\mathbf{H}} = &- t \sum_{i\neq j,\sigma} \hat{a}^{\dagger}_{i\sigma}\hat{a}_{j\sigma} + U\sum_{i} \hat{n}_{i\uparrow}\hat{n}_{i\downarrow} + \frac{U'}{2}\sum_{i\neq j,\sigma,\sigma'} \hat{n}_{i\sigma}\hat{n}_{j\sigma'} \\ &- J_{pair}\sum_{i\neq j} \hat{a}^{\dagger}_{i\uparrow}\hat{a}^{\dagger}_{i\downarrow}\hat{a}_{j\uparrow}\hat{a}_{j\downarrow} + \frac{J_{Hund}}{2}\sum_{i\neq j,\sigma,\sigma'} \hat{a}^{\dagger}_{i\sigma}\hat{a}^{\dagger}_{j\sigma'}\hat{a}_{i\sigma'}\hat{a}_{j\sigma} \\ &+ \sum_{k} \Delta(\hat{n}_{k\uparrow} + \hat{n}_{k\downarrow})\end{aligned} \tag{1}$$

From the fundamentals of physics, we know that equal charges repel. As a result, configurations where two electrons occupy the same orbital lead to an increased energy. This is exactly where we introduce our first static parameter U. This parameter represents the Coulomb potential between two particles in a single orbital. Mathematically, the term can be described by the following particle number operators: $U \cdot \hat{n}_{im\uparrow}\hat{n}_{im\downarrow}$. In this research we will also consider the Coulomb potential between two particles in different orbitals on a single site. This potential is denoted by U'. The Coulomb potential between different sites is neglected.

Next we will introduce the kinetic interaction t. This is the hopping parameter. It represents the hopping of an electron from one orbital to another. In the Hubbard model, the hopping parameter is described by the following term: $t \cdot \hat{a}^{\dagger}_{im\sigma}\hat{a}_{jm'\sigma}$. A configuration where hopping is possible, is energetically more favorable. This can again be understood from a charge based argument. The possibility of hopping increases the electron's delocalization. Accordingly, the electron's charge density is smaller. Such a decrease in charge density is energetically favored.

We will now introduce Hund's exchange mechanism J_{Hund}. This exchange takes on three different forms. Firstly, we have the pair exchange, where a pair of electrons hops from one orbital to another. This exchange will be denoted by J_{pair}, however for this research the value is equal to that of J_{Hund}.
Secondly, we have Hund's exchange for anti-parallel spins, which occurs when two anti-parallel spins exist in different orbitals.
Lastly, we have Hund's exchange for parallel spins. This case occurs when we have two parallel spins in different orbitals. These three exchanges can be found in table 1. Here, they are represented by their mathematical form, together with a schematic illustration.

Table 1: All three variants of Hund's exchange, together with their mathematical form and a schematic representation.

Pair exchange	$J_{pair} \cdot \hat{a}^\dagger_{im\uparrow}\hat{a}^\dagger_{im\downarrow}\hat{a}_{im'\uparrow}\hat{a}_{im'\downarrow}$	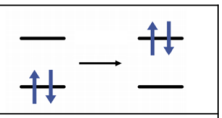
Anti-parallel spin exchange	$J_{Hund} \cdot \hat{a}^\dagger_{im\sigma}\hat{a}^\dagger_{im'\sigma'}\hat{a}_{im\sigma'}\hat{a}_{im'\sigma}$	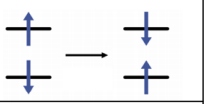
Parallel spin exchange	$J_{Hund} \cdot \hat{a}^\dagger_{im\sigma}\hat{a}^\dagger_{im'\sigma}\hat{a}_{im\sigma}\hat{a}_{im'\sigma}$	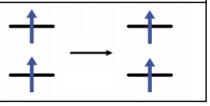

The parallel spin exchange is especially interesting, since it results in a decreased energy, while it leaves the configuration effectively invariant. Due to this invariance, the parallel spin exchange can be interpreted as a decrease of the intra-orbital Coulomb potential U'. This property will become clearly visible in the discussion of the matrix in section 3.1.

Before we start constructing this Hamiltonian, we need to introduce the final parameter Δ. This parameter represents the energy difference between different orbitals. It can be interpreted as the cost for an electron to occupy an energetically higher orbital. For example, electrons that occupy d-orbitals pay an energetic penalty compared to electrons that occupy p-orbitals. In this case, the energy difference is denoted by Δ_{pd}. We will also include the Δ-parameter for the energy difference between different d-orbitals. In this case, the parameter represents the crystal field splitting. We will explicitly deal with two types of d-orbitals on the Chromium sites, so called t2g-and eg-orbitals. In this consideration, the eg-orbitals are placed at a higher energy. The summation in the last term of equation 1 would therefore run over all eg-orbitals.

2.3 Triqs

For the computational analysis of the Hubbard model simulations, the Triqs programming toolbox was used [4]. Triqs can be used to perform the exact diagonalization of second quantization operator Hamiltonians like equation 1. This diagonalization yields the energy eigenvalues for all possible eigenstates. When the full set of eigenstates is acquired, this also allows us to determine the eigenvalues of other observables. For this project, we are interested in the magnetic ordering of the system. Therefore, we will consider the eigenvalues of the spin operators $\hat{S}_z$ and $\hat{S^2}$. The spin operators can be expressed in terms of second quantization operators. This derivation follows from the Pauli-matrix representation of the operators [5].

$$\begin{aligned}
\hat{S}^x_{im} &= \frac{1}{2}\left(\hat{a}^\dagger_{im\uparrow}\hat{a}_{im\downarrow} + \hat{a}^\dagger_{im\downarrow}\hat{a}_{im\uparrow}\right) \\
\hat{S}^y_{im} &= -\frac{i}{2}\left(\hat{a}^\dagger_{im\uparrow}\hat{a}_{im\downarrow} - \hat{a}^\dagger_{im\downarrow}\hat{a}_{im\uparrow}\right) \\
\hat{S}^z_{im} &= \frac{1}{2}\left(\hat{n}_{im\uparrow} - \hat{n}_{im\downarrow}\right)
\end{aligned} \tag{2}$$

From these operators, we can construct $\hat{S^2} = S_x^2 + S_y^2 + S_z^2$. Calculating the eigenvalues of this operator allows us to distinguish between singlet and triplet states. Together with the energy eigenvalues, we can determine the energy difference $\Delta E = E_{singlet} - E_{triplet}$ between the lowest singlet and triplet states. This observable ΔE serves as a measure for the magnetic coupling of the system. When this coupling is positive, we find a singlet ground state. Hence the spins are not aligned, and the system behaves antiferromagnetically. When the magnetic coupling is negative, the ground state forms a triplet. Hence, the spins are aligned and the system behaves ferromagnetically.

3 Simulations

In this section we will discuss four different models. We will start with a detailed description of a rather simple system. Next we will discuss the Kugel-Khomski direct exchange model and the Goodenough-Kanamori indirect exchange model. Finally we introduce the full model, together with its properties and Hamiltonian.

3.1 Two-site Hubbard model

Let us start by reconsidering the two-site Hubbard model. This model is the simplest representation of the interaction between two Chromium sites. This minimal description only contains a single orbital per Chromium site. In practise, we expect the two orbitals to have equal energies. However, for the sake of completeness, the two involved orbitals are placed at different energy levels. As a result, we need to take the Δ-parameter into account. For this research, we will consider the relevant configurations, where the system is half-filled. Hence, the system is occupied by a total of two electrons.

The full Hilbert space of a half-filled two-site Hubbard model can be split into two subspaces. The first subspace consists of four basis vectors with a total spin of zero. The potentials and exchange mechanisms are represented in matrix 3. The second subspace consists of two basis vectors with a total spin of 1. This results in matrix 4. This simplification can be performed since all considered interactions conserve the total spin.

$$\mathbf{H} = \begin{pmatrix} U & J_{pair} & -t & +t \\ J_{pair} & U+2\Delta & -t & +t \\ -t & -t & U'+\Delta & J_{Hund} \\ +t & +t & J_{Hund} & U'+\Delta \end{pmatrix} \begin{matrix} |\uparrow\downarrow,\cdot\rangle \\ |\cdot,\uparrow\downarrow\rangle \\ |\uparrow,\downarrow\rangle \\ |\downarrow,\uparrow\rangle \end{matrix} \tag{3}$$

$$\mathbf{H} = \begin{pmatrix} U'-J_{Hund}+\Delta & 0 \\ 0 & U'-J_{Hund}+\Delta \end{pmatrix} \begin{matrix} |\uparrow,\uparrow\rangle \\ |\downarrow,\downarrow\rangle \end{matrix} \tag{4}$$

These matrices can of course be diagonalized. This can be done numerically, for example by using the 'Numpy Linalg' package. While somewhat tedious, even the analytical derivation of the eigenvalues is fairly straightforward.

This system can also be represented in terms of the second quantization operators introduced in section 2.2. This results in the following Hamiltonian [5][6].

$$\begin{aligned}\hat{\mathbf{H}} = &- t \sum_{i \neq j,\sigma} \hat{a}^\dagger_{i\sigma} \hat{a}_{j\sigma} + U \sum_i \hat{n}_{i\uparrow} \hat{n}_{i\downarrow} + \frac{U'}{2} \sum_{i \neq j,\sigma,\sigma'} \hat{n}_{i\sigma} \hat{n}_{j\sigma'} \\ &- J_{pair} \sum_{i \neq j} \hat{a}^\dagger_{i\uparrow} \hat{a}^\dagger_{i\downarrow} \hat{a}_{j\uparrow} \hat{a}_{j\downarrow} + \frac{J_{Hund}}{2} \sum_{i \neq j,\sigma,\sigma'} \hat{a}^\dagger_{i\sigma} \hat{a}^\dagger_{j\sigma'} \hat{a}_{i\sigma'} \hat{a}_{j\sigma} \\ &+ \Delta(\hat{n}_{2\uparrow} + \hat{n}_{2\downarrow})\end{aligned} \tag{5}$$

This Hamiltonian is equivalent to that of equation 1, however we now specifically have one orbital at a higher energy than the other. Therefore, the operators of the form $\hat{n}_{2\sigma}$ work on the orbital which is placed at a higher energy.

It is important to note that, in contrast to the matrices, this operator Hamiltonian is not limited to an occupation of two electrons. Hence, the diagonalization of equation 5 yields the eigenvalues for all possible occupations. It should also be mentioned that the exact diagonalization of equation 5 in Triqs is essentially an equivalent procedure to the analytical derivation of the above matrices.

3.2 Kugel-Khomski direct exchange model

We will now consider the direct interaction between the Chromium sites. For this discussion we again construct a system of two Chromium sites. However, we now include two orbitals per site. Hence, our system contains a total of four orbitals. A schematic overview of this situation can be found in figure 2. Including a second orbital for each Chromium site adds an extra level of complexity, since the system now contains different possible hopping interactions. First, we include hopping between two orbitals on the same site: $t_{ii}^{mm'}$ where $m \neq m'$. Secondly we include hopping between the same orbitals on different sites: t_{ij}^{mm} where $i \neq j$. Lastly, we include hopping between different orbitals on different sites: $t_{ij}^{mm'}$ where both $i \neq j$ and $m \neq m'$. The t2g-and eg-orbitals are denoted by $m = 1$ and $m = 2$ respectively.

Figure 2: Schematic overview of two Chromium sites, each containing a lower t2g-orbital and a higher eg-orbital with a crystal field splitting Δ.

For the sake of simplicity, we neglect all Coulomb potentials and Hund's exchange mechanisms between the two different sites. This approximation is justifiably, since the actual parameter values quickly decrease over longer distances. As a result of this approximation, t_{ij}^{mm} and $t_{ij}^{mm'}$ are the only inter-site interactions.

The direct exchange Hamiltonian is closely related to equation 5. The main difference is the addition of a second orbital on each Chromium site. Using the notation introduced above, we can construct the following Hamiltonian:

$$\begin{aligned}\hat{\mathbf{H}} = &- \sum_{i,j,m,m',\sigma} t_{ij}^{mm'} \hat{a}_{im\sigma}^{\dagger} \hat{a}_{jm'\sigma} (1 - \delta_{ij}\delta_{mm'}) \\ &+ U \sum_{i,m} \hat{n}_{im\uparrow} \hat{n}_{im\downarrow} \\ &+ \frac{U'}{2} \sum_{i,m\neq m',\sigma,\sigma'} \hat{n}_{im\sigma} \hat{n}_{im'\sigma'} \\ &- J_{pair} \sum_{i,m\neq m'} \hat{a}_{im\uparrow}^{\dagger} \hat{a}_{im\downarrow}^{\dagger} \hat{a}_{im'\uparrow} \hat{a}_{im'\downarrow} \\ &+ \frac{J_{Hund}}{2} \sum_{i,m\neq m',\sigma,\sigma'} \hat{a}_{im\sigma}^{\dagger} \hat{a}_{im'\sigma'}^{\dagger} \hat{a}_{im\sigma'} \hat{a}_{im'\sigma} \\ &+ \Delta \sum_{i} (\hat{n}_{i2\uparrow} + \hat{n}_{i2\downarrow})\end{aligned} \tag{6}$$

In this Hamiltonian, each individual Chromium site contains the same interactions as considered in section 3.1. The additional hopping parameters have been included via the matrix $t_{ij}^{mm'}$. The diagonalization of this Hamiltonian again results in the eigenvalues for all possible occupations. For this research, we will consider the case where the t2g-orbitals are half-filled. Hence the system still contains a total of two electrons.

For the Kugel-Khomski direct exchange model, we can determine an effective prediction for the magnetic coupling [2][6][7]. The expression for this coupling is constructed by taking the limit of large U, and downfolding the Hilbert space into parts containing the relevant singlet and triplet states. This general procedure can be found in [5].

$$J_{ij} = \frac{4 \cdot I^a}{U} - \frac{4 \cdot I^f \cdot J_{Hund}}{(U + \Delta)(U + \Delta - J_{Hund})} \tag{7}$$

Where J_{ij} can be interpreted as the exchange coupling for an effective spin model. It is equivalent to the energy difference $\Delta E = E_{singlet} - E_{triplet}$ proposed in section 2.3. In this equation $I^a = (t_{ij}^{mm})^2$ is the square of the hopping parameter between the same orbitals on different sites. Similarly, $I^f = (t_{ij}^{mm'})^2$ is the square of the hopping parameter between different orbitals on different sites.

In this expression, the first term describes the antiferromagnetic behaviour, and the second term describes the ferromagnetic behaviour. Hence, when $J_{ij} > 0$ or $J_{ij} < 0$ we find that the behaviour of the ground state is respectively antiferromagnetic or ferromagnetic. An important aspect of this result is that the leading order of the ferromagnetic term scales with $\sim \frac{1}{U^2}$. In contrast, the antiferromagnetic term scales with $\sim \frac{1}{U}$. In the relevant working regime, i.e. for large Coulomb interactions U and U' compared to hopping t and Hund's exchange J_{Hund}, the predicted magnetic coupling is therefore always antiferromagnetic ($J_{ij} > 0$).

3.3 90° indirect exchange model

We will now study the Goodenough-Kanamori indirect exchange, where the interaction between the Chromium sites is mediated by the Iodide ligands. For the considerations of this interaction, we approximate the angle of the Cr-I-Cr chain to be 90°. The simplest 90-degree indirect exchange model consists of four orbitals. Two of these orbitals are d-orbitals (Chromium) and the remaining two are p-orbitals (Iodide). When we consider the indirect exchange, there is no direct hopping between the two d-orbitals. As a result, there is no direct communication between the Chromium sites. Their interaction is, however, mediated by the Iodide ligands between the Chromium sites. An important characteristic of the 90-degree symmetry is that due to the orthogonality of the p-orbitals, electrons in one p-orbital are unable to reach the other p-orbital [8]. Hence, there is no hopping between the p_x-and p_y-orbitals. This includes the hopping t, but also the pair hopping J_{pair}. A second result of the 90-degree symmetry, is that each d-orbital only interacts with the closest p-orbital. Consequently, the entire system can be separated into two equivalent systems, both consisting of a single d-orbital, and its neighboring p-orbital. The only interaction between these two systems is Hund's exchange on the Iodide ligand J_{xy}. A schematic overview of the full situation can be found in figure 3.

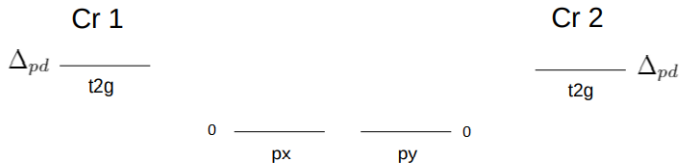

Figure 3: Schematic overview of two Chromium sites, with one d-orbital per site. Between the Chromium sites lies an Iodide ligand containing two orthogonal p-orbitals.

In this model, both the Coulomb potential on the Chromium sites U_d and the energy difference between the p- and d-orbitals Δ_{pd} are large compared to the other parameters. As a result, the p-orbitals will be fully occupied. Furthermore, we still consider the situation where the Chromium sites are half-filled. Hence, we have a total of six electrons occupying the system.

We are still mainly interested in the magnetic coupling, and thus the energy difference between the singlet and triplet states. For this reason, together with the fact that the p-orbitals will be fully occupied, we do not need to take any coulomb potentials on the p-orbitals into account.

Due to the symmetry of the model, we conclude that the hopping parameter between p- and d-orbitals is equal on the left and right side of the system. We therefore introduce the following notation: $t_{d1,px} = t_{d2,py} = t_{pd}$. Using this notation, the Hamiltonian becomes the following.

$$\begin{aligned}\hat{\mathbf{H}} = &- t_{pd} \sum_{\sigma} (\hat{a}^{\dagger}_{d_1\sigma}\hat{a}_{p_x\sigma} + \hat{a}^{\dagger}_{p_x\sigma}\hat{a}_{d_1\sigma} + \hat{a}^{\dagger}_{d_2\sigma}\hat{a}_{p_y\sigma} + \hat{a}^{\dagger}_{p_y\sigma}\hat{a}_{d_2\sigma}) \\ &+ U_d \sum_i \hat{n}_{d_i\uparrow}\hat{n}_{d_i\downarrow} \\ &+ \frac{J_{xy}}{2} \sum_{i\neq j,\sigma,\sigma'} \hat{a}^{\dagger}_{p_i\sigma}\hat{a}^{\dagger}_{p_j\sigma'}\hat{a}_{p_i\sigma'}\hat{a}_{p_j\sigma} \\ &+ \Delta_{pd} \sum_i (\hat{n}_{d_i\uparrow} + \hat{n}_{d_i\downarrow})\end{aligned} \tag{8}$$

The matrix-Hamiltonian of this indirect model is constructed by E. Koch [5]. In this matrix, Koch did not include any Hund's exchange terms for p-orbitals which are doubly occupied. His reasoning is based on the particle-hole symmetry. A state with three electrons in two orbitals is equivalent to the existence of

one hole. Hence, this state cannot exhibit any interactions where two particles are exchanged. For the anti-parallel spin exchange, this restriction is included in the operators. i.e. the anti-parallel spin exchange results in the creation of two electrons with identical quantum numbers. This term therefore automatically vanishes, since it leads to a violation of Pauli's principle. The parallel spin exchange on the other hand, is not restricted by the operator nature. This exchange can be manually excluded for double occupations by the addition of $(1-\hat{n}_{p_x\uparrow}\hat{n}_{p_x\downarrow})(1-\hat{n}_{p_y\uparrow}\hat{n}_{p_y\downarrow})$ terms. We have decided not to include such terms, as they seem very unnatural. We did find that the inclusion of these terms would result in a deviation of about 10% on the final result for the magnetic coupling. The discussion about this detail is currently unresolved.

For the indirect exchange, we can again determine an effective equation for the magnetic coupling. Such a prediction can be derived by downfolding the full Hilbert space, and expanding the Hamiltonian in $\frac{1}{U_d}$. This approximation is thus again valid for large values of U. More details on the explicit derivation can be found in [5]. The effective magnetic coupling becomes:

$$J = -\frac{4t_{pd}^4}{(U_d+\Delta_{pd})^2}\frac{2J_{xy}}{4(U_d+\Delta_{pd})^2 - J_{xy}^2} \tag{9}$$

Note that this equation is strictly negative. This predicts the ferromagnetic behavior of the 90-degree indirect exchange model.

3.4 Full model

The full model consists of six orbitals. The p_x and p_y-orbitals still form the center of the system at a 90-degree angle. Therefore, similar to section 3.3, hopping between the p_x and p_y orbitals is still prohibited. However, we now combine the direct exchange interactions from section 3.2 with the indirect exchange from section 3.3. A schematic overview of the full model can be found in figure 4.

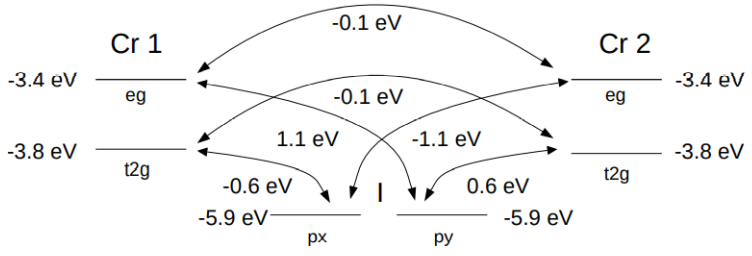

Figure 4: Schematic overview of the orbital manifold containing four Chromium d-orbitals and two Iodide p-orbitals. The hopping parameter values and energy levels are explicitly given.

As seen in figure 4, a number of interactions have been neglected for the sake of simplicity. This approximation is justified for the specific case of CrI_3, since the parameter values that follow from first principle calculations were relatively small. The remaining relevant interactions are the direct hopping interactions between equal orbitals on the different Chromium sites, and the indirect exchange interaction which is still mediated by the Iodide ligand. In this indirect interaction, the lower orbital mainly couples to the closest p-orbital, while the upper orbital predominantly couples to the opposing p-orbital. Due to the simplicity of this model, We can easily identify both the direct interactions and the indirect interactions. The interplay between these two channels will be investigated by again constructing an operator Hamiltonian.

The operator terms from equation 6 in the direct exchange model can be directly implemented. On the other hand, the Hamiltonian for the indirect exchange in equation 8 needs to be adjusted. This is due to the fact that the full model contains two d-orbitals per Chromium site, while the indirect model only considers one. Implementing all interactions appropriately results in the following Hamiltonian.

$$
\begin{aligned}
\hat{\mathbf{H}} = &- \sum_{i,j,m,m',\sigma} t_{ij}^{mm'} \hat{a}^\dagger_{d_{im}\sigma} \hat{a}_{d_{jm'}\sigma} (1 - \delta_{ij}\delta_{mm'}) \\
&- t_{pd} \sum_{\sigma} (\hat{a}^\dagger_{d_{11}\sigma} \hat{a}_{p_x\sigma} + \hat{a}^\dagger_{p_x\sigma} \hat{a}_{d_{11}\sigma} + \hat{a}^\dagger_{d_{12}\sigma} \hat{a}_{p_y\sigma} + \hat{a}^\dagger_{p_y\sigma} \hat{a}_{d_{12}\sigma}) \\
&- t_{pd} \sum_{\sigma} (\hat{a}^\dagger_{d_{21}\sigma} \hat{a}_{p_y\sigma} + \hat{a}^\dagger_{p_y\sigma} \hat{a}_{d_{21}\sigma} + \hat{a}^\dagger_{d_{22}\sigma} \hat{a}_{p_x\sigma} + \hat{a}^\dagger_{p_x\sigma} \hat{a}_{d_{22}\sigma}) \\
&+ U_{d,t2g} \sum_i \hat{n}_{d_{i1}\uparrow} \hat{n}_{d_{i1}\downarrow} + U_{d,eg} \sum_i \hat{n}_{d_{i2}\uparrow} \hat{n}_{d_{i2}\downarrow} + \frac{U'_d}{2} \sum_{i,m\neq m',\sigma,\sigma'} \hat{n}_{d_{im}\sigma} \hat{n}_{d_{im'}\sigma'} \\
&- J_{pair} \sum_{i,m\neq m'} \hat{a}^\dagger_{d_{im}\uparrow} \hat{a}^\dagger_{d_{im}\downarrow} \hat{a}_{d_{im'}\uparrow} \hat{a}_{d_{im'}\downarrow} \\
&+ \frac{J_{Hund}}{2} \sum_{i,m\neq m',\sigma,\sigma'} \hat{a}^\dagger_{d_{im}\sigma} \hat{a}^\dagger_{d_{im'}\sigma'} \hat{a}_{d_{im}\sigma'} \hat{a}_{d_{im'}\sigma} \\
&+ \frac{J_{xy}}{2} \sum_{i\neq j,\sigma,\sigma'} \hat{a}^\dagger_{p_i\sigma} \hat{a}^\dagger_{p_j\sigma'} \hat{a}_{p_i\sigma'} \hat{a}_{p_j\sigma} \\
&+ \Delta_d \sum_i (\hat{n}_{d_{i2}\uparrow} + \hat{n}_{d_{i2}\downarrow}) + \Delta_{pd} \sum_{i,m} (\hat{n}_{d_{im}\uparrow} + \hat{n}_{d_{im}\downarrow})
\end{aligned}
\tag{10}
$$

Note that in this Hamiltonian we introduce different parameters for the Coulomb potential on the t2g-orbitals $U_{d,t2g}$ and the potential on the eg-orbitals $U_{d,eg}$. The d-orbitals itself are labeled by d_{im}, where $i = 1, 2$ runs over the two Chromium sites, and the t2g-and eg-orbitals are represented by $m = 1$ and $m = 2$ respectively.

4 Results

The full set of parameter values for CrI_3 is given by table 2. These parameter values have been previously acquired by DFT calculations[9].

Table 2: All nearest neighbour parameter values for the full Hubbard model of CrI_3.

Parameter	Value (eV)
$t_{ii}^{mm'}$	0
t_{ij}^{mm}	0.1
$t_{ij}^{mm'}$	0
t_{pd}	0.6
$U_{d,t2g}$	4.0
$U_{d,eg}$	4.2
U'_d	3.2
J_{pair}	0.5
J_{Hund}	0.5
J_{xy}	0.2
Δ_{pd}	2.1
Δ_d	0.4

These parameters will be used explicitly for the direct, indirect and the full model. The discussion of the simple two-site Hubbard model will serve as an introduction to the interplay between the hopping parameter and Hund's exchange.

4.1 Two-site Hubbard model

In section 3.1 we introduced the two-site Hubbard model. This model consisted of two sites, each containing a single orbital. For the simple case where $U = U' > 0$, and $\Delta = 0$, we find a very clear interplay between the hopping t(antiferromagnetic) and Hund's exchange J_{Hund}(ferromagnetic). This result can be seen in figure 5.

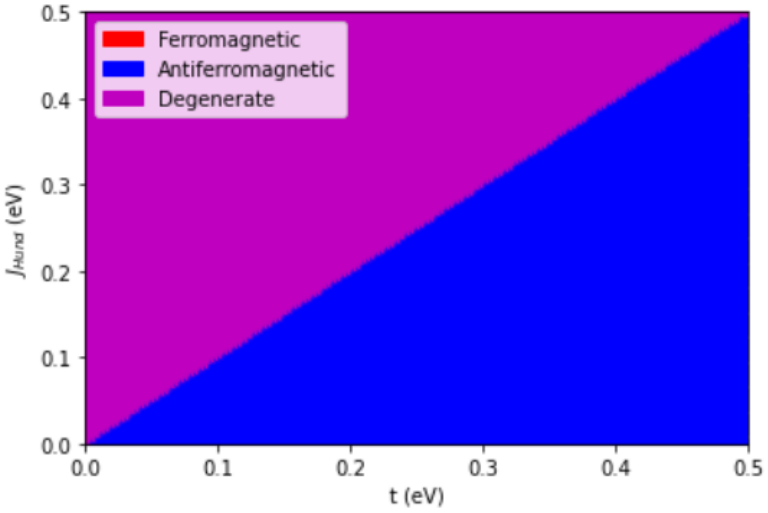

Figure 5: Magnetic phase diagram for the ground state of a half-filled two-site Hubbard model, for any arbitrary $U = U' > 0$ and $\Delta = 0$.

In the region where the hopping parameter t is dominant, the ground state is a singlet. Hence the hopping leads to an antiferromagnetic coupling. When Hund's exchange J_{Hund} is dominant, we find that the singlet and the triplet are degenerate. This degeneracy is due to the simplicity of the parameter set. For this set, the different Hund's exchanges have equal contributions to the energy.

When $\Delta \neq 0$, and $U > U'$, the overall result becomes less trivial. The transition boundary changes, and the degeneracy is lifted. When $\Delta < U - U'$, the ferromagnetic behavior becomes more dominant. This behavior can be seen in figure 6. In the opposite case, when $\Delta > U - U'$, the behavior becomes more antiferromagnetically dominant.

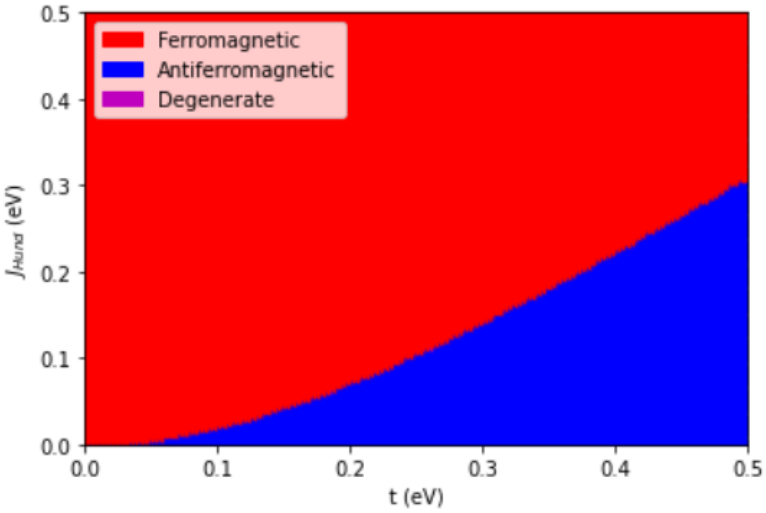

Figure 6: Magnetic phase diagram for the ground state of a half-filled two-site Hubbard model, for the case where $U = 4eV$, $U' = 3eV$ and $\Delta = 0.5eV$.

Due to the simplicity of the two-site model, the result of the simulation in Triqs was easily validated by obtaining the eigenvalues of matrix 3 numerically.

The important take-away from this simple model, is that when the hopping parameter is dominant, we find an antiferromagnetic singlet ground state, while a dominant Hund's exchange leads to a ferromagnetic triplet ground state.

4.2 Kugel-Khomski direct exchange model

In section 3.2 we introduced the direct exchange model which contains two Chromium sites, with two d-orbitals per site. For the relevant regime, the exact diagonalization of this model always yields a singlet ground state. Therefore, the ground state of the direct exchange model always behaves antiferromagnetically. The results are shown in more detail in figure 7. For the sake of validation, we have taken $U_{d,t2g} = U_{d,eg} = U$ as the main variable. Varying U implies that U' must vary accordingly. For this purpose, the identity $U' = U - 2J_{Hund}$ was used [10]. All other parameters were kept constant.

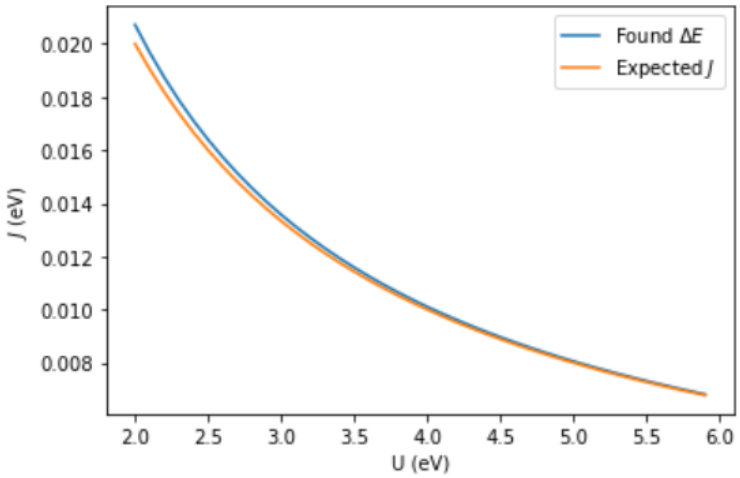

Figure 7: Graph representing the expected magnetic coupling J (orange), together with the determined energy difference between the lowest singlet and triplet state ΔE (blue) for the direct exchange model. The varied parameter is the Coulomb potential U.

For large values of U, we find a near perfect correspondence between the expectation following from equation 7 and the result of the exact diagonalization. For smaller values of U, we find a small deviation. This deviation can be explained by the fact that equation 7 is an effective equation, which is only valid for large values of U.

From section 3.2 we know that the direct model revolves around the direct hopping between the Chromium sites. We see a clear correspondence with the results in section 4.1. This simple two site Hubbard model showed that when the hopping parameter is dominant, the overall behaviour of the model is antiferromagnetic. This is reflected in the antiferromagnetic behaviour of the direct model.

For the exact parameters of CrI_3, i.e. at a value of $U = 4.2$ eV, the direct model finds a magnetic coupling of $J = 10$ meV. Hence, the model finds antiferromagnetism, while we expect ferromagnetism. The found value of the magnetic coupling is also an order of magnitude too large, since the actual value is $J \approx -1$ meV[2].

4.3 90° Indirect exchange model

in section 3.3 we introduced the indirect exchange model which consists of two Chromium sites with a single Iodide ligand. This model contains a single d-orbital per Chromium site, and two orthogonal p-orbitals on the Iodide ligand. The ground state for this Indirect exchange model is always found to be a triplet. Therefore the ground state always behaves ferromagnetically. This result is portrayed in more detail in figure 8.

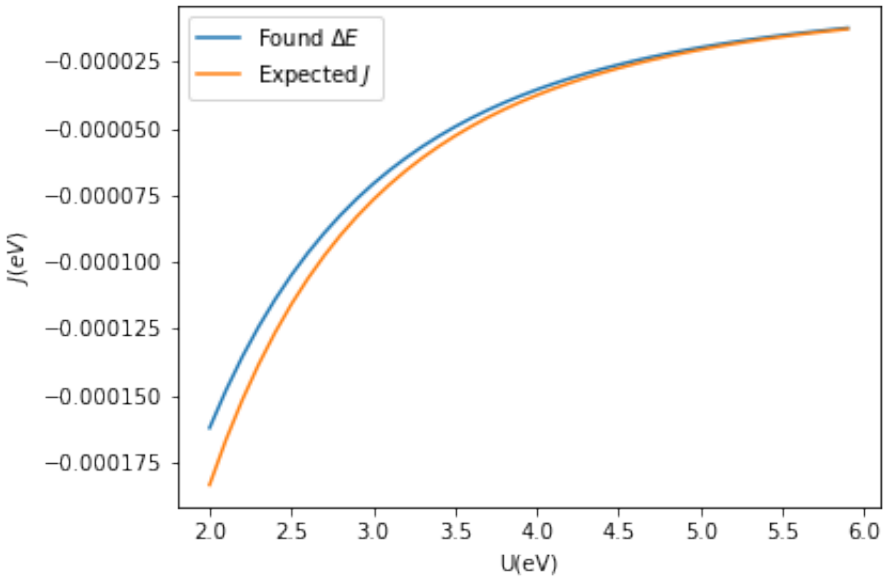

Figure 8: Graph containing the expected magnetic coupling J (orange), together with the determined energy difference between the lowest singlet and triplet state ΔE (blue) for the indirect exchange model. The varied parameter is the Coulomb potential U.

The correspondence between the expected magnetic coupling J from equation 9 and the values acquired from the exact diagonalization is similar to that of section 4.2. We again find a near perfect match for large values of U, while the result deviates for smaller values of U. The reason for this deviation is also similar, since the equation for the expected magnetic coupling is again an effective equation, which is only applicable for large values of U.

From section 3.3 we know that for the indirect exchange model, the only interaction between the Chromium sites is mediated via Hund's exchange. This is again in good agreement with the results found for the simple two-site Hubbard model in section 4.1, which also found a ferromagnetic ground state for the regime where J_{Hund} is the dominant parameter.

For the exact parameters of CrI_3 (i.e. at a value of $U = 4.2$ eV), we find a magnetic coupling of $J = -0.0375$ meV. Hence, the model finds the correct ferromagnetic behaviour. However, the found value of the magnetic coupling is nearly two orders of magnitude too small.

4.4 Full model

The exact diagonalization of the full model described in section 3.4 can find both a singlet or a triplet ground state. The model therefore contains the ability to describe both ferromagnetism and antiferromagnetism. This phase transition is visible in figure 9. The inter-and intra-Coulomb potentials are varied similar to section 4.2.

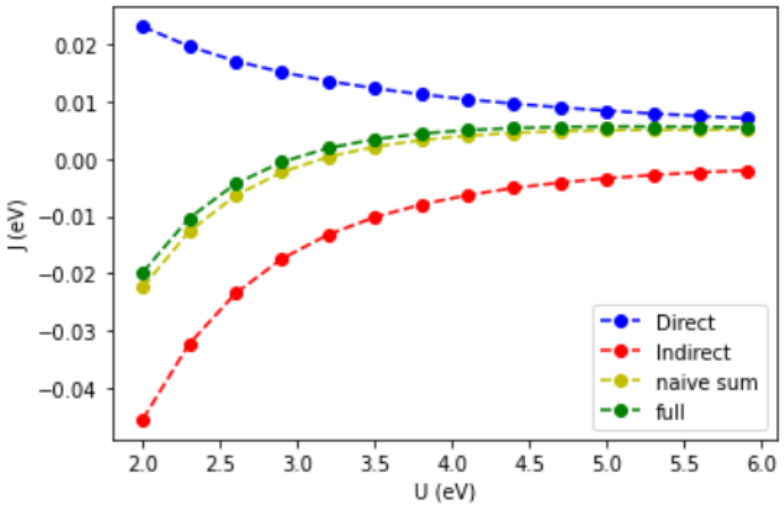

Figure 9: Graph of the magnetic coupling of the full model, together with coupling of the individual direct and indirect channels, which are found within the full model. A naive sum of these channels is included for reference. The varied parameter is the coulomb potential U.

The first important observation comes from the comparison of the indirect channel within the full model in figure 9 to the actual model of the indirect exchange in figure 8. The difference between these two situations has been briefly mentioned in section 3.4: the full model contains two d-orbitals per Chromium site, while the indirect model only contains one. From the figures, we find that the dependence of the magnetic coupling on the Coulomb potential is unchanged. However, the magnetic coupling is nearly two orders of magnitude larger when the additional d-orbitals are included.

A second observation comes solely from figure 9. We find that the full model behaves very closely to the naive sum of the individual channels. Hence, the interplay between the direct and indirect channels is rather limited.

For the exact parameter set of CrI_3 (i.e. at $U = 4.2$ eV), we find a magnetic coupling of $J = 5.17$ meV. Even though this still predicts antiferromagnetism, the magnitude of the magnetic coupling is closer to the actual value than either of the individual models.

5 Conclusion

We have constructed a model which contains both direct and indirect exchange mechanisms. First we analysed these mechanisms separately. From figure 7 we conclude that a model which consists solely of direct exchange mechanisms can only predict antiferromagnetic behaviour. Hence this model can never provide a complete description of reality. The same argument holds for a model which only contains indirect exchanges. This can be seen in figure 8, which shows the strictly ferromagnetic behaviour of the indirect model.

The combination of direct and indirect exchanges yields a model which finds both ferro-and antiferromagnetism. This transistion was found in figure 9. This figure also showed the near additive interplay between both exchange channels. This characteristic causes the model to give an insightful and intuitive description of the magnetic behaviour. When a certain parameter set results in either ferromagnetism or antiferromagnetism, this can be related to the dominance of the indirect or direct channel respectively. From this dominance, we can straightforwardly pinpoint the exact interaction from which this behaviour originates.

The value of the magnetic coupling for CrI_3 found in section 4.4 is $J = 5.17$meV. The actual nearest neighbour magnetic coupling of CrI_3 is found to be of the order of $J \approx -1$ meV [2]. Hence, on a quantitative level, the model is not fully reliable. However, compared to the individual models, we now find a description which qualitatively fits better to previous research.

6 Discussion

The current model contains a number of approximations, and is still very minimalistic. The diagonalization of the full Hamiltonian can be performed in less than five minutes. Therefore, there is still some room for the implementation of additional complexity. In this section, we will discuss the main approximations of the model, and give hypotheses for the impact of these approximations.

6.1 Second ligand

In this research, we have only considered a single Iodide ligand. From figure 1, we know that two Chromium sites are actually connected by two ligands. An important addition to the model would therefore be the implementation of this second ligand. This would simply be the addition of a second, equivalent, indirect exchange channel. The simplest expectation for this expansion would be that the magnetic coupling of the indirect channel in figure 9 now becomes twice as large. The direct exchange channel would however remain invariant. Hence, assuming the model still behaves closely to the naive sum, we expect the result of the full simulation to be shifted into the ferromagnetic region.

6.2 Neglected parameters

As briefly discussed in section 3.4, a number of interactions have been neglected. The reason for this approximation was simply due to the relatively small parameter values. A few of these neglected parameters could however be somewhat relevant. For example, hopping between the Chromium t2g-orbital and the opposite p-orbital is found to have a value of 0.15-0.19 eV [9]. Another neglected parameter with probable relevance is the hopping between the Chromium eg-orbital and the closest p-orbital. This interaction is found to have a value of 0.1-0.17 eV [9]. We can give a superficial prediction for the implementation of these additional hopping interactions. Since we now include more hopping between the Chromium sites and the Iodide ligands, the coupling between these orbitals will become stronger. Therefore, we expect the indirect channel to become more dominant, and thus we expect the magnetic coupling to decrease.

When these small hopping parameters are included, one must at some point also consider the long range Coulomb and Hund-interactions. However, we need to first calculate these parameter values, before we can make a proper statement about their relevance.

6.3 90° assumption

In section 3.3, we argued that the 90° symmetry causes the p-orbitals on the Iodide ligand to be orthogonal. As a result, we did not include any hopping from the p_x to the p_y orbital. When we consider the lattice structure of CrI_3 in figure 1, the angle of the Cr-I-Cr bond is actually closer to 93° [3]. This

slightly larger angle would allow for a small amount of hopping between the two p-orbitals, $t_{p_x-p_y} = 0.108$eV [9]. This would essentially be the addition of a third channel, the 180° indirect exchange. This exchange is known to couple antiferromagnetically [5]. Hence, we expect a certain competition between the 90° channel and the 180° channel. This competition could potentially lead to a slight increase of the magnetic coupling. Thus making the result more antiferromagnetic.

6.4 Nearest neighbours

As mentioned in section 2.1, this research only considers nearest neighbour interactions. Including more than two Chromium sites in the model will drastically increase the complexity. On top of that, these additional interactions will be between much more spatially separated sites. Hence, the parameter values are likely to be relatively small. It is therefore questionable whether the increased precision weighs up to the loss of insightfulness.

6.5 Additional orbitals

So far, we have included a maximum of two orbitals per Chromium site. In reality, each Chromium site contains three t2g-orbitals and two eg-orbitals. In section 4.4, we found that the magnetic coupling of the indirect exchange is nearly two orders of magnitude larger when we consider two orbitals per Chromium site instead of one. Due to this observation, it would be interesting to see how the result changes with the implementation of even more additional d-orbitals.

References

[1] B. Huang et al, Layer-dependent ferromagnetism in a van der Waals crystal down to the monolayer limit, *Nature* **546** 270 (2017)

[2] I.V. Kashin et al *2D Mater.* **7** 025036 (2020)

[3] J.L. Lado and J. Fernández-Rossier *2D Mater.* **4** 035002 (2017)

[4] O. Parcollet, M. Ferrero, T. Ayral, H. Hafermann, I. Krivenko, L. Messio, and P. Seth, *Comp. Phys. Comm.* **196** 398-415 (2015)

[5] E. Pavarini, E. Koch, R. Scalettar, and R. Martin (eds.) The Physics of Correlated Insulators, Metals, and Superconductors. *Modeling and Simulation* Vol. **7** (2017)

[6] V.V. Mazurenko, F. Mila and V.I. Anisimov, *Phys. Rev.* B **73** 014418 (2006)

[7] K.I. Kugel and D.I. Khomski *Sov. Phys. Usp.* **25** 231 (1982)

[8] J. Kanamori, *J. Phys. Chem. Solids* **10** 87-98 (1959)

[9] D. Soriano, A.N. Rudenko, M.I. Katsnelson, and M. Rösner. Environmental Screening and Ligand-Field Effects to Magnetism in CrI3 Monolayer. (arXiv:2103.04686) (2021)

[10] C. Lacroix, *J. Phys.* C **13** 5125 (1980)